Universality and Hysteretic Dynamics in Rapid Fracture

A. Livne, G. Cohen, and J. Fineberg

The Racah Institute of Physics, The Hebrew University of Jerusalem, Jerusalem 91904, Israel

(Received 14 March 2005; published 10 June 2005)

Experiments in the dynamic fracture of brittle polyacrylamide gels show that a single-crack state undergoes a hysteretic transition to the microbranching instability with a characteristic activation time. Quantitative measurements also indicate that features such as crack front inertia, self-focusing of microbranches, and the appearance of front waves are universal attributes of dynamic fracture.

DOI: 10.1103/PhysRevLett.94.224301 PACS numbers: 62.20.Mk, 46.50.+a, 47.54.+r

The study of rapid fracture dynamics has been the subject of much recent interest [1–4]. Much of this is related to the nature and origin of the microbranching instability, in which a propagating crack becomes unstable to ''frustrated'' crack branching [1]. Many important attributes of fracture dynamics remain unresolved as experiments are hampered by the difficult problem of visualizing the small region at the tip of a crack that is moving at velocities that approach material sound speeds. We overcome this problem by the use of brittle polyacrylamide gels, ''soft'' materials in which sound speeds are 2–3 orders of magnitude lower than in ''standard'' brittle materials.

We first use gels to establish the universality of many features of the microbranching instability. These include ''3D'' effects such as the acquisition of inertia by cracks [5], the formation of front waves [6], and the self-focusing of microbranches in the direction normal to crack motion. Previously observed solely in glass, these effects cannot be described within current theories [1,2,7], which assume that fracture takes place within 2D media. We then use this system to extend our knowledge of fracture dynamics. We show that the microbranching instability both behaves like a first-order phase transition and possesses a characteristic activation time scale, which becomes apparent only at high acceleration rates. These observations may provide a key to understanding persistent gaps between quantitative theoretical predictions and experimental observations.

Gels have been previously used to study fracture at [8] and near [9] the onset of propagation. Polyacrylamide gels are highly tunable, soft media composed of cross-linked polymer chains immersed in an aqueous solution. The concentrations of the monomers (acrylamide) and cross-linking molecules (bisacrylamide) determine their elastic properties [10]. The gels were cast to 0.05 cm thick (Z direction) sheets of typical ($X \times Y$) 5×5 cm^2 dimensions, where we define X and Y as, respectively, the propagation and loading directions. Casting was performed by polymerizing the gel between clamped glass plates separated by a Mylar spacer. After polymerization, gels were left for over 24 h in an aqueous salt solution with Bromophenol Blue dye to facilitate visualization and render the gels electrically conductive.

Most of our experiments were performed on brittle gels composed of 13.8% (w/v) acrylamide and 2.6% bisacrylamide whose shear and extensional waves speeds are, respectively, 5.3 ± 0.1 (measured) and 10.7 ± 0.2 m/s (calculated). The Poisson ratio of 0.5 yields a Rayleigh wave speed, V_R, of 5.1 m/s. Polyacrylamide gels (at room temperatures) are neo-Hookean elastomers [11]. At the 10% strains used in our experiments [Fig. 1(b)] their behavior is nearly linear elastic with a Young's modulus of 87 ± 4 kPa. Experiments in other concentrations (e.g., 23% acrylamide, 10% bisacrylamide) produced similar results.

The gel sheets were loaded in a mode I configuration [Fig. 1(a)] by uniform displacement of their vertical (Y direction) boundaries. One vertical edge of the gel is attached to a precision translational stage, while the opposing edge is attached to a load cell, to measure the applied stress. A small ''seed'' crack is introduced either at the sample's edge or center, midway between the vertical boundaries. The gel edges were displaced quasistatically until arriving at a desired strain (typically 5%–15%). Electrodes, inserted at either side of the crack, were used to measure the potential drop during the crack propagation. The potential drop was monitored via an ac bridge, driven at 800 kHz, and demodulated by a Matec 605 analog demodulator. Both the direct demodulated signals and their analog derivatives were sampled at a 10 MHz/12 bit resolution. To minimize any drying effects, experiments were

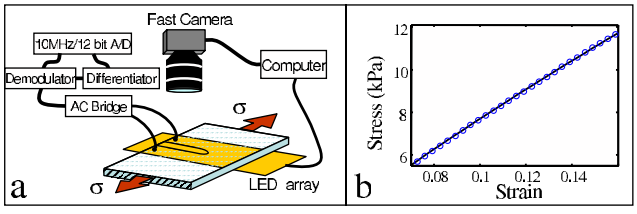

FIG. 1 (color online). (a) Schematic diagram of the experimental system. (b) The measured (circles) and theoretical (line) [11] stress-strain relation of polyacrylamide gels in the range of strains over which our experiments were performed yield a shear modulus of 28 kPa ± 1.

conducted minutes after taking the gels out of the dye-salt solution.

Fracture was initiated by gently sharpening the seed crack with a scalpel. The crack's instantaneous location and profile were monitored by both the potential drop method and direct visualization via a (VDS CNC1300) high speed camera set to a spatial resolution of 1280×192 lines. Stroboscopic lighting of the gel sample using an ultrabright light emitting diode array enabled multiple exposures within each frame, capturing crack profiles every 0.25–1.5 mm of the crack extension at frame rates between 2500–5000 frames/s. At the end of each run the fracture surface was analyzed via an optical microscope interfaced to a computer.

The typical dynamic behavior of a crack is shown in Fig. 2(a). In this experiment the crack accelerates smoothly until $v_c = 0.34V_R$ (more on the value of v_c later), leaving in its wake a flat, mirrorlike, surface. At $0.34V_R$ a small drop in the crack's speed is recorded, which is accompanied with the appearance of a chain of distinct, kite-shaped surface markings [Fig. 2(a) (inset) and Fig. 2(b)]. Rapid oscillations now appear in the crack's velocity as the fracture surface becomes increasingly rougher. The velocity oscillations are correlated with microbranch formation, with each dip (peak) in the velocity corresponding to a rougher (smoother) surface section.

The above dynamics mirror the onset of the microbranching instability [1,5] observed in the tensile fracture of glass and poly(methyl methacrylate) (PMMA). Beyond respective critical velocities of $0.42V_R$ and $0.36V_R$ in these materials, a single-crack state no longer exists. Instead,

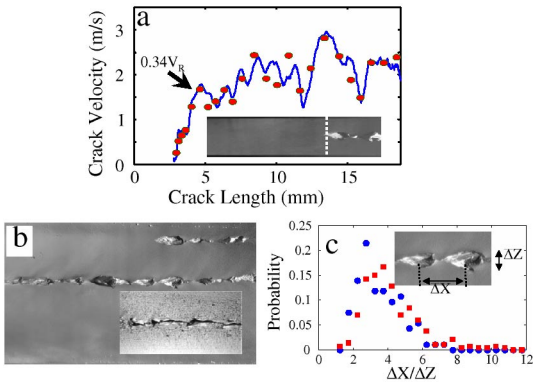

FIG. 2 (color online). (a) A typical measurement of the crack velocity, v, using both visualization (circles) and the potential drop method, averaged over 0.4 ms (line). (inset) A photograph of a 1.5×0.5 mm^2 section of the corresponding fracture surface at the onset of the microbranching instability (dashed line) at $v_c = 0.34V_R$. (b) Photographs of branch lines (chains of successive microbranches) on fracture surfaces of a 2 mm thick gel and (inset) soda-lime glass. (c) Comparison of the branch-line scaling in 23% acrylamide and 10% bisacrylamide gels (squares) and glass (circles). In both materials the ratios of ΔX, the distance between successive branches with their thickness, ΔZ, are nearly identically distributed. All cracks shown propagate from left to right.

microscopic cracks, called microbranches, evolve and branch away from the main crack, tracing out a spoonlike contour. In these materials the microbranch "backbone" was found to obey a power-law form $Y \propto X^{0.7}$, where X and Y are, respectively, the directions parallel and perpendicular to the direction of propagation of the main crack, whose origin is the point of microbranch initiation. Profiles consistent with this form have also been theoretically predicted [12]. In gels the microbranches follow a nearly identical power-law profile of $Y \propto X^{\alpha}$ with $\alpha = 0.75 \pm 0.05$. Thus, the instability in polyacrylamide gels which, at the microscopic level are very different from both glass and PMMA, is nearly identical to that observed in the other materials.

For $v > v_c$ microbranches are not dispersed at random over the fracture surface. Instead, they are highly localized in the Z direction and, as in glass [6,13], created one after another in directed lines called "branch lines" [Fig. 2(b)] [14]. A closer inspection of the internal branch-line structure in [Fig. 2(c)] reveals that the width ΔZ and spacing ΔX between the craters created by the microbranches are related. Measurements of the ratio $\Delta X/\Delta Z$ reveal nearly identical distributions in gels and glass with a mean value of 4 ± 1. An interesting difference between both materials is that, whereas in gels $0.02 < \Delta Z < 0.2$ mm, observed values of ΔZ in glass span nearly 3 orders of magnitude. In addition, branch lines of many different scales are often interspersed [6] in glass. In gels of up to thickness 2 mm, we have rarely observed more than three simultaneous branch lines.

The existence of a critical velocity for the creation of branch lines having the same scaling and nontrivial structure in these highly different materials is a strong indication of the universality of these effects in dynamic fracture. The observation that microbranches occur only in chains within a highly focused branch-line structure is indicative of the acquisition of inertia by a crack; each microbranch is triggered by the preceding one, suggesting that the crack front retains a "memory." Neither these inertial effects nor the focusing in Z, which conserves the width of a given branch line, are described in current (2D) theoretical descriptions of dynamic fracture. These nontrivial dynamics suggest that theories of fracture may need to be significantly modified to accommodate them.

Further evidence of 3D effects in fracture is the appearance of front waves, when translational invariance in Z is broken. Front waves are nonlinear, solitary waves that travel along the leading edge of a propagating crack and leave visible tracks on the fracture surface. They have, until now, been directly observed only in glass [5,6]. Figure 3 shows that these waves also exist in gels which, as in glass, can be generated by microbranch formation along a branch line. The angle α formed by the tracks (inset of Fig. 3) relative to the propagation direction is related [5,15,16] to the front wave velocity, V_{FW}, via $v = V_{\mathrm{FW}} \cos(\alpha)$. Using the measured instantaneous velocity, v, a constant value of V_{FW} is obtained whose value of $0.95 \pm 0.03V_R$ is in ex-

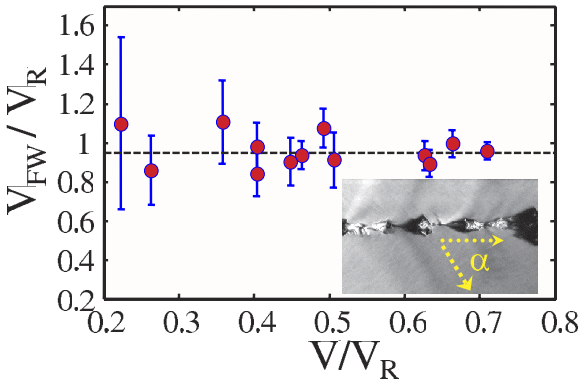

FIG. 3 (color online). The front wave velocity [5], $V_{\mathrm{FW}} = v/\cos(\alpha)$, as calculated from measured values of v and α (see inset), normalized by V_R. As predicted in [16], $V_{\mathrm{FW}} = 0.95V_R$ with a 95% confidence interval of ± 0.03. The inset (of height 0.45 mm) shows typical front waves in gels which, as in glass, are generated by microbranch formation.

cellent agreement with the values $0.94V_R < V_{\mathrm{FW}} < V_R$ predicted in [16]. This strengthens the evidence [17] for the existence of front waves in dynamic fracture. Front waves in gels decay more rapidly than in glass. This suggests that the fracture energy in gels is a slowly increasing function of velocity [16], in contrast to its nearly constant value in glass [5].

Let us now look again at the value of v_c, the critical velocity for microbranching. When a crack accelerates slowly [e.g., Fig. 2(a)], v_c is typically $\sim 0.34V_R$, which is close to the value measured in PMMA. Values of v_c in this range are generally observed when a crack is driven with quasistatic loading. When fracture is initiated from the center of a sample, however, two counterpropagating cracks will be initiated at different times, due to slight asymmetries in the initial seed crack. The acceleration of the first crack will be comparable to cracks with quasistatic loading. The second crack, loaded by both the external stress and stress changes induced by the first crack, can experience acceleration rates an order of magnitude higher. As Fig. 4(a) shows, v_c systematically increases from $0.34V_R$ (1.7 m/s) at acceleration rates, $a \sim 200$ m/s^2, to values as high as $0.75V_R$ (3.8 m/s) for $a \sim 4000$ m/s^2. The roughly linear increase in v_c with a suggests a mean activation time, $\tau \sim 0.5$ ms, for the instability. Similar effects in glass (extension of the mirror region to $0.97V_R$ under shock loading) have been noted in [13].

The apparent "scatter" evident in Fig. 4(a) is far larger than our measurement error of ± 0.2 m/s. Thus, the activation times are not constant but follow a distribution. Measurements of the time interval between the moment when v surpasses $0.34V_R$ until the appearance of the first microbranch indicate that the activation times are both independent of a and are [Fig. 4(b)] consistent with an exponential distribution having mean (0.6 ms) and decay (0.5–1 ms) times close to the activation time provided by the slope of Fig. 4(a).

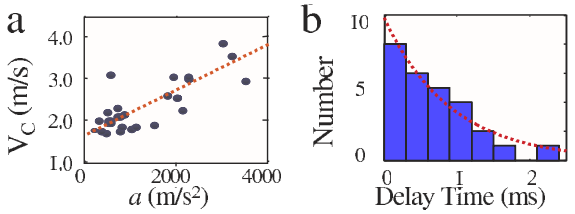

FIG. 4 (color online). (a) The critical velocity, v_c, for the onset of microbranches increases systematically with the mean acceleration, a, over the range $0.34V_R < v_c < 0.75V_R$ (where $0.34V_R$ is the minimum observed value of v_c). The slope of a linear fit (line) yields a characteristic "activation" time of $\tau = 0.5$ ms. (b) Histogram of the time intervals between $v = 0.34V_R$ and v_c. The mean value of these activation times, 0.6 ms, is consistent with the value of τ derived from (a).

Let us now consider the spatially localized form of branch lines. Spatially localized states are formed in many driven dissipative systems that experience the rapid nonlinear growth which drives a first-order phase transition. Localized states typically occur in the hysteretic region, where either of two different states can be stable. Spatial localization occurs when these bistable states coexist in different spatial domains, which are formed when nonlinear growth is balanced by mechanisms such as dissipation, dispersion, or the existence of a globally conserved quantity [18].

In this picture, branch lines, embedded in the surrounding "mirror" region, can be viewed as coexisting single-crack and multiple-crack states. Hysteresis between these two states is a necessary condition for spatial localization by this mechanism. To examine this possibility, we performed experiments in which the sample was loaded with a linearly decreasing strain as a function of x. Under this loading, the initial crack is very rapid and microbranching states quickly form. The crack then gradually slows until the microbranching state undergoes a reverse transition to a single-crack state. As demonstrated in Fig. 5, the reverse transition is clearly hysteretic, occurring at a velocity which is significantly below the critical velocity $v_c > 0.34V_R$ for the forward transition. Further evidence of bistability is provided by the existence of transient patches of mirrorlike surfaces in regions where v is well beyond v_c. Branch-line widths systematically increase with v until the onset of large-scale branching, when ΔZ approaches the sample width.

In light of this clear hysteresis, the minimal observed value of v_c (1.7 m/s) may simply be indicative of the intrinsic noise level within the system (e.g., vibrations induced by the loading). This picture would predict a distribution of the activation times which is similar to Fig. 4(a). Once within the bistable regime, the instability may be triggered when random perturbations surpass a critical threshold for triggering the first microbranch [19]. This would yield a finite probability to bifurcate at each time interval after the minimum ($0.34V_R$) value of v_c and produce an exponential distribution similar to Fig. 4(b).

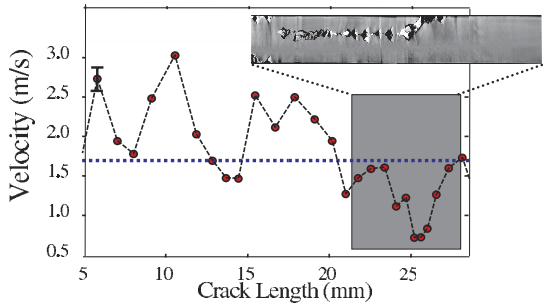

FIG. 5 (color online). The microbranching instability is hysteretic with v. Shown is a typical plot of v as a function of the crack length, L, as the imposed strain driving the crack is decreased with L. Although the onset from a single crack to microbranching occurs at $v_c > 1.7$ m/s $= 0.34V_R$ (dotted line), the reverse transition back to a single-crack state occurred only for $v < 0.15v_c$. Despite the fact that v in the shaded region is significantly below v_c, the corresponding fracture surface (inset photograph of the 0.5 mm thick surface between $22.1 < L < 27.2$ mm) shows pronounced microbranching. Note that the velocity fluctuations are caused by the microbranches and are far larger than our measurement error.

In conclusion, we have first shown that many features of the dynamics of the brittle fracture of polyacrylamide gels are identical to those observed in standard brittle materials, thus making a strong case for their universality. We then demonstrated that, in gels, cracks undergo a hysteretic transition from a single-crack to a multiple-crack state. This transition may explain the spatially confined nature of the branch lines as well as the activation time distribution for the instability onset. We should note that, although clearly observed in the gels, these properties have not yet been observed in other materials, with hysteresis in glass not visible within the 10% measurement resolution of our preliminary experiments.

Bistability of single-crack and multiple-crack states could resolve quantitative discrepancies between experiments and theoretical models, which predict [12,20–22] significantly higher values of v_c [23]. Energetic barriers [12,24] to the transition between single and branched states are circumvented due to the strong localization in the Z direction of the branch lines, which occupy only a fraction of the fracture surface. Both this strong localization and persistence (inertia) of the branch lines indicate that the energy flowing to the crack must be inhomogeneously distributed in Z throughout the sample thickness. The activation time, τ, could have its origin in the time required to establish this inhomogeneous stress field. These important and, possibly, interrelated issues all lack theoretical explanations and present a challenge to our fundamental understanding of the fracture process.

We gratefully acknowledge J. Bechhoefer for suggesting polyacrylamide to us. This research was supported by the Israel Science Foundation (Grant No. 194/02).

[1] J. Fineberg and M. Marder, Phys. Rep. **313**, 1 (1999).
[2] I. S. Aranson, V. A. Kalatsky, and V. M. Vinokur, Phys. Rev. Lett. **85**, 118 (2000); H. Henry and H. Levine, Phys. Rev. Lett. **93**, 105504 (2004); A. Karma and A. E. Lobkovsky, Phys. Rev. Lett. **92**, 245510 (2004).
[3] J. F. Boudet, S. Ciliberto, and V. Steinberg, J. Phys. II (France) **6**, 1493 (1996); J. A. Hauch and M. P. Marder, Int. J. Fract. **90**, 133 (1998).
[4] M. J. Buehler, F. F. Abraham, and H. J. Gao, Nature (London) **426**, 141 (2003).
[5] E. Sharon, G. Cohen, and J. Fineberg, Nature (London) **410**, 68 (2001).
[6] E. Sharon, G. Cohen, and J. Fineberg, Phys. Rev. Lett. **88**, 085503 (2002).
[7] L. B. Freund, *Dynamic Fracture Mechanics* (Cambridge University Press, Cambridge, 1990).
[8] D. Bonn, H. Kellay, M. Prochnow, K. Ben-Djemiaa, and J. Meunier, Science **280**, 265 (1998); L. Benguigui, Physica (Amsterdam) **270A**, 1 (1999).
[9] Y. Tanaka, K. Fukao, Y. Miyamoto, H. Nakazawa, and K. Sekimoto, J. Phys. Soc. Jpn. **65**, 2349 (1996).
[10] R. Nossal, Rubber Chem. Technol. **61**, 255 (1988).
[11] L. R. G. Treloar, *The Physics of Rubber Elasticity* (Oxford University Press, New York, 1975), 3rd ed.; M. Marder, Phys. Rev. Lett. **94**, 048001 (2005).
[12] M. Adda-Bedia, J. Mech. Phys. Solids **53**, 227 (2005); E. Bouchbinder, J. Mathiesen, and I. Procaccia, Phys. Rev. E (to be published).
[13] E. K. Beauchamp, J. Am. Ceram. Soc. **78**, 689 (1995).
[14] Features, coined ''river patterns,'' resembling branch lines were observed in [9], but no direct velocity or subsurface measurements were performed.
[15] J. W. Morrissey and J. R. Rice, J. Mech. Phys. Solids **46**, 467 (1998).
[16] S. Ramanathan and D. S. Fisher, Phys. Rev. Lett. **79**, 877 (1997).
[17] D. Bonamy and K. Ravi-Chandar, Phys. Rev. Lett. **91**, 235502 (2003); E. Sharon, G. Cohen, and J. Fineberg, Phys. Rev. Lett. **93**, 099601 (2004).
[18] H. Riecke, *Localized Structures in Pattern-Forming Systems in Pattern Formation in Continuous and Coupled Systems*, edited by M. Golubitsky, D. Luss, and S. Strogatz, IMA Vol. 115 (Springer, New York, 1999), p. 215.
[19] L. M. Sander and S. V. Ghaisas, Phys. Rev. Lett. **83**, 1994 (1999).
[20] M. Marder and S. Gross, J. Mech. Phys. Solids **43**, 1 (1995).
[21] E. H. Yoffe, Philos. Mag. **42**, 739 (1951).
[22] D. A. Kessler and H. Levine, Phys. Rev. E **59**, 5154 (1999).
[23] Alternative explanations, based on the dynamics of the process zone, have been proposed in M. Adda-Bedia, M. Ben Amar, and Y. Pomeau, Phys. Rev. E **54**, 5774 (1996); H. Gao, J. Mech. Phys. Solids **44**, 1453 (1996); and [2].
[24] J. D. Eshelby, Sci. Prog. **59**, 161 (1971).